Journal of Quantitative Spectroscopy & Radiative Transfer 130 (2013) 341–351

Contents lists available at ScienceDirect

Journal of Quantitative Spectroscopy & Radiative Transfer

journal homepage: www.elsevier.com/locate/jqsrt

Terahertz spectroscopy of hydrogen sulfide

Ala'a A.A. Azzam [a], Sergei N. Yurchenko [a], Jonathan Tennyson [a,*], Marie-Aline Martin-Drumel [b,c,1], Olivier Pirali [b,c]

[a] Department of Physics and Astronomy, University College London, London WC1E 6BT, UK
[b] CNRS, UMR 8214, Institut des Sciences Moléculaires d'Orsay, Université Paris Sud XI, Orsay, F-91405 Orsay, France
[c] Synchrotron SOLEIL, AILES beamline, F-91192 Gif-Sur-Yvette, France

ARTICLE INFO

Article history:
Received 7 March 2013
Received in revised form
28 May 2013
Accepted 30 May 2013
Available online 11 June 2013

Keywords:
Hydrogen sulfide
Line assignments
Atmospheric physics
Planetary atmospheres

ABSTRACT

Pure rotational transitions of hydrogen sulfide (H_2S) in its ground and first excited vibrational states have been recorded at room temperature. The spectrum comprises an average of 1020 scans at 0.005 cm^{-1} resolution recorded in the region 45–360 cm^{-1} (1.4 to 10.5 THz) with a globar continuum source using a Fourier transform spectrometer located at the AILES beamline of the SOLEIL synchrotron. Over 2400 rotational lines have been detected belonging to ground vibrational state transitions of the four isotopologues $H_2{}^{32}S$, $H_2{}^{33}S$, $H_2{}^{34}S$, and $H_2{}^{36}S$ observed in natural abundance. 65% of these lines are recorded and assigned for the first time, sampling levels as high as $J=26$ and $K_a=17$ for $H_2{}^{32}S$. 320 pure rotational transitions of $H_2{}^{32}S$ in its first excited bending vibrational state are recorded and analysed for the first time and 86 transitions for $H_2{}^{34}S$, where some of these transitions belong to new experimental energy levels. Rotational constants have been fitted for all the isotopologues in both vibrational states using a standard effective Hamiltonian approach. Comprehensive comparisons are made with previously available data as well as the data available in HITRAN, CDMS, and JPL databases. The 91 transitions assigned to $H_2{}^{36}S$ give the first proper characterization of its pure rotational spectrum.

1. Introduction

Hydrogen sulfide (H_2S) is produced naturally in volcanoes [1] and is a byproduct of human activity such as water treatment processes [2]; it is therefore a trace species in the Earth's atmosphere. It is known to be more abundant in the atmospheres of solar system gas giants [3] and it is thought to be important for the sulfur chemistry of extra-solar planets [4]. Indeed it is also found in the atmospheres of cool stars and is the dominant sulfur-bearing gas-phase species in substellar objects such as brown dwarfs [3]. H_2S has long been known to be present in interstellar clouds in our galaxy [5] and has also been observed in starburst galaxies [6]. Its role in shocks and star formation regions is thought to be of particular importance [7]. Modern astronomical telescopes such as Herschel, SOFIA and ALMA have allowed astronomers to observe species such as H_2S at THz frequencies for the first time [8], thus opening a window on higher-lying rotational levels for this species.

H_2S is a light nonrigid molecule with C_{2v} symmetry. This molecule has three vibrational modes: two overlapped stretching, symmetric (ν_1) and asymmetric (ν_3) respectively at 2615 and 2626 cm^{-1}, and one bending (ν_2) at 1183 cm^{-1}. H_2S is a near oblate asymmetric top rotor with $\kappa = 0.52$. Four sulfur isotopes are stable: ^{32}S, ^{33}S, ^{34}S, and ^{36}S with natural abundances of 95.02%, 0.75%, 4.21% and 0.02% respectively.

Since the work of Burrus and Gordy [9], numerous studies of H_2S rotational transitions in the ground vibrational state in the region up to about 9.3 THz (310 cm^{-1})

* Corresponding author. Tel.: +44 20 7679 7809.
E-mail address: j.tennyson@ucl.ac.uk (J. Tennyson).
[1] Present address: Laboratoire de Physico-Chimie de l'Atmosphère, EA 4493, Université du Littotal Côte d'Opale, F-59140 Dunkerque, France.

0022-4073/$ - see front matter © 2013 Published by Elsevier Ltd.
http://dx.doi.org/10.1016/j.jqsrt.2013.05.035

have been performed. In the microwave region, 82 lines have been detected for the main isotopologue ($H_2{}^{32}S$) [9–15], 40 transitions for $H_2{}^{34}S$ [9,10,12,16], 155 transitions for $H_2{}^{33}S$ with hyperfine splitting due to ^{33}S nucleus [9,16], and three experimental transitions for $H_2{}^{36}S$ as well [16]. In the far infrared (FIR), 443 observed transitions have been reported for $H_2{}^{32}S$ [17–19,15], 71 transitions for $H_2{}^{33}S$ [18], and 173 transitions for $H_2{}^{34}S$ [18].

Particularly important for this work are the measurements by Flaud et al. [18], who probed the region below 9.3 THz, and of Yamada and Klee [19], who made measurements in the same region. Frequencies from these two works in addition to the available experimental microwave data, and effective Hamiltonian fits to them, provide the rotational spectra used in recent editions of HITRAN [20,21] and JPL [22] databases. However rotational frequencies beyond 10 THz are estimated by extrapolating these formula. In CDMS database [23,24], the pure rotational transitions have been calculated using all the available measured transitions in the microwave and FIR region. We note that the higher rotational states of H_2S are also of interest theoretically [25].

Many other studies have been performed in order to detect the absorption transitions of H_2S molecule and its isotopologues ($H_2{}^{33}S$ and $H_2{}^{34}S$) in its fundamental, hot, and combination vibrational bands covering the spectrum range up to 16 500 cm^{-1}. The most important for this work are the transitions in the fundamental bending mode (ν_2) [26–29]. Among these studies, Ulenikov et al. [29] reported the most accurate experimental upper state energy levels in ν_2 band for $H_2{}^{32}S$, $H_2{}^{33}S$, and $H_2{}^{34}S$.

In this work we present new experimental measurements of the spectrum of hydrogen sulfide in the region 1.4–10.5 THz (45–360 cm^{-1}). This work is a byproduct of our work in order to produce a complete hot line list of H_2S [30]. The following section gives experimental details. Section 3 presents the analysis of our new frequencies. In Section 4 a comprehensive comparison with the previous measurements is presented.

2. Experiments

The Fourier transform FIR absorption spectrum of gas phase H_2S in natural abundance was recorded using a globar source available on the Bruker IFS125 interferometer of the AILES beamline at the SOLEIL synchrotron [31]. A resolution of 0.005 cm^{-1} was used to record the spectrum in the spectral range 45–360 cm^{-1}. A pressure of 0.16 mbar of H_2S was injected in a room-temperature White-type cell aligned for an optical path length of 150 m. The interferometer was pumped to a pressure below 10^{-4} mbar using a turbomolecular pump; two polypropylene windows were used to separate the interferometer from the absorption cell. The resulting spectrum is the coaddition of 1020 scans (about 12 hours of acquisition time). Fig. 1 shows an overview of the recorded spectrum, while Fig. 2 gives an illustrative region containing newly observed lines.

Spectral calibration was performed using the residual water transitions and the accurate transition frequencies of Refs. [32,33]. A calibration curve was prepared to facilitate correction of the recorded frequencies for H_2S. Fig. 3 shows the dispersion of the water transitions before and after the calibration. The accuracy of the line position is thus estimated to be 0.0005 cm^{-1}.

3. Spectral analysis

Lines for H_2S molecule with intensities above 10^{-25} $cm^{-1}/(molecule \times cm^{-2})$ were detected for the region above 80 cm^{-1}. In the region below 50 cm^{-1} only lines with intensity above 10^{-23} $cm^{-1}/(molecule \times cm^{-2})$ were detected as a consequence of the nature of the spectrum obtained from the blackbody radiator: the low intensity of

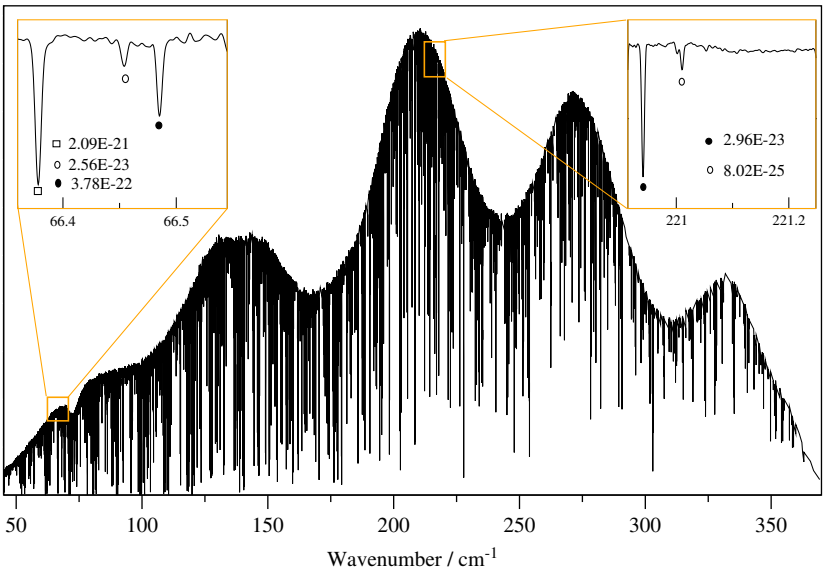

Fig. 1. Room temperature absorption spectrum of H_2S recorded at AILES beamline. The insets illustrate detection of different line intensities for two sample regions of the spectrum. The numbers next to the symbols give the intensities of the lines in $cm^{-1}/(molecule \times cm^{-2})$ according to HITRAN [21].

the light leads to a limited signal-to-noise ratio which decreases fastly below 50 cm^{-1} as seen in Fig. 1. Examples of line detections with different intensities in the different regions of the spectrum are given in the same figure.

The absorption spectrum was analysed manually by matching lines with the available data in the HITRAN database [21] and the CDMS database [23,24] for the main isotopologue for the vibrational ground state transitions.

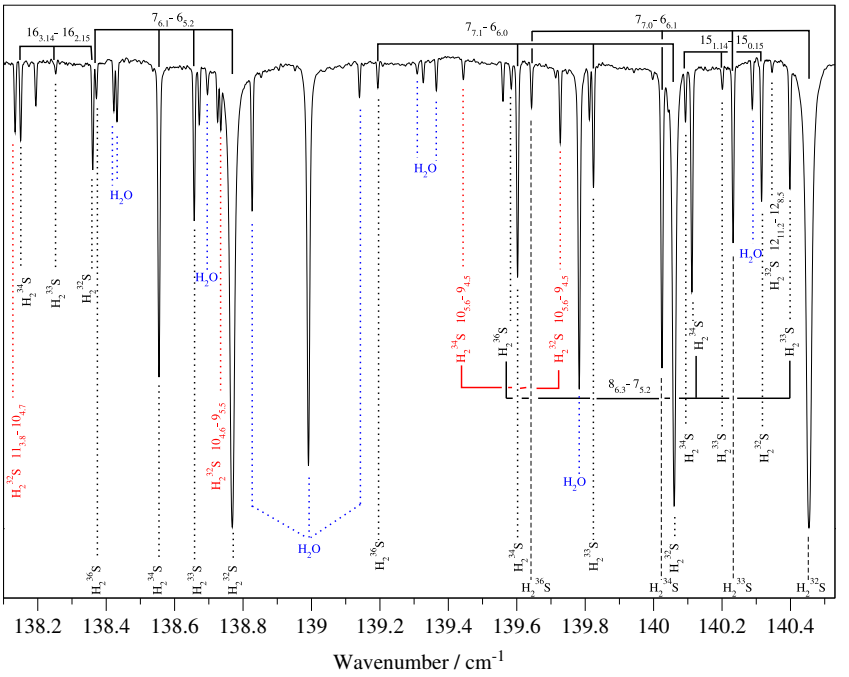

Fig. 2. A portion of the absorption spectrum of H_2S recorded at SOLEIL, showing some pure rotational transitions in both ground and bending vibrational states $v_2 = 1$. The pure rotational transitions of $v_2 = 1$ are illustrated in red color. (For interpretation of the references to color in this figure caption, the reader is referred to the web version of this article.)

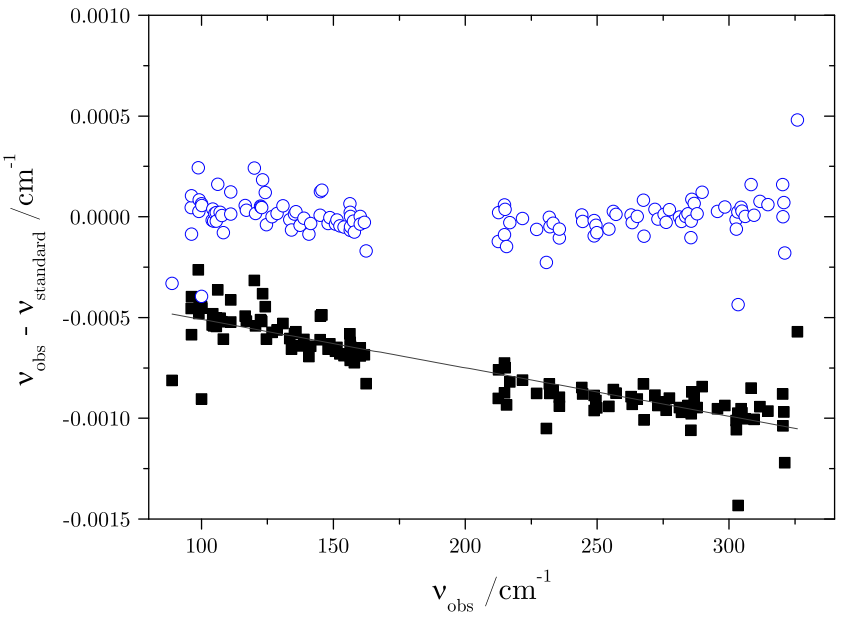

Fig. 3. Calibration of the FIR Fourier transform spectrum recorded in this work. Water line positions before calibration (■) and after calibration (○) based on the accurate water line positions of Refs. [32,33]. The line equation in cm^{-1} is $d = -2.40(12)\nu - 2.69(26)$, where d is the dispersion and ν is the transition frequency. The standard deviation after calibration is 1.05×10^{-4} cm^{-1}.

While for $H_2{}^{33}S$ and $H_2{}^{34}S$ in their vibrational ground state, the HITRAN database was used. For the $H_2{}^{36}S$ isotopologue, many transitions were identified and assigned manually by extrapolating the line positions of the three other isotopologues for given quantum numbers, see Fig. 2. The pure rotational transitions of the vibrational state $\nu_2=1$ of $H_2{}^{32}S$ were initially assigned using a variational line list calculated using the DVR3D variational nuclear motion program [34]. This line list will be published elsewhere [30]. Experimental upper energy levels belong to ν_2 band given by Ulenikov et al. [29] were used to calculate the pure rotational transitions in the $\nu_2=1$ state for $H_2{}^{32}S$ and $H_2{}^{34}S$. These calculated transitions were used to confirm the assignments for $H_2{}^{32}S$ and to identify pure rotational transitions for $H_2{}^{34}S$.

Pickett's program CALPGM [35] was used to fit the observed spectra for each of the four isotopologues in both states of this molecule studied in this work. Table 1 summarises the number of the fitted parameters and the number of the spectral lines used in the fit for each isotopologue in both vibrational states. For $H_2{}^{32}S$ in the ground vibrational state, the 926 newly recorded lines were combined with 462 lines of Helminger et al. [13], Belov et al. [15], and Yamada and Klee [19]. The resulting fit parameters were used to predict 2919 transitions for $H_2{}^{32}S$ in the ground vibrational state up to $J=30$ and $K_a=20$. For $H_2{}^{34}S$, 576 of our measured lines were combined with 40 lines from Saleck et al. [16] and Huiszoon and Dymanus [36] to fit 41 parameters. Using the fitted parameters, a pure rotational spectrum was

Table 1
Summary of the fits for the four isotopologues of H_2S in the ground and first bending vibrational states with a comparison with the previous works for the same molecule.

Reference	Method	Vib. state	ISO	MW lines		IR lines		Parameters	RMS		σ[c]
				Previous	Recorded	Previous	Recorded		MW(MHz)	IR (cm^{-1})	cm^{-1}
Flaud et al. [18]	A-I[r]	000	$H_2{}^{32}S$	39 [9,13,10,12]	–	–	387	29	0.25	0.00035	0.0008
			$H_2{}^{33}S$	1 [9,12]	–	–	71	8	–	0.00031	0.0008
			$H_2{}^{34}S$	2 [9,12]	–	–	173	15	–	0.00025	0.0010
Yamada and Klee [19]	S-I[r]	000	$H_2{}^{32}S$	40 [13,14]	–	–	376	30	82	0.000213	0.0007
Belov et al. [15]	Padé-I[r]	000	$H_2{}^{32}S$	29 [13,14]	64	376 [19]	30	24	366	0.000265	0.0003
Saleck et al. [16]	A-I[r]	000	$H_2{}^{33}S$	–	155	71 [18]	–	37[a]			
			$H_2{}^{34}S$	2 [12]	38	173 [18]	–	28			
This work	S-I[r]	000	$H_2{}^{32}S$	82 [13,15]	–	380 [15,19]	926	44	0.339	0.00046	
			$H_2{}^{33}S$	155 [16]	–	–	433	34[a]	0.258	0.00046	
			$H_2{}^{34}S$	40 [16,36]	–	–	576	41	0.063	0.00047	
			$H_2{}^{36}S$	1 [16]	–	–	91	24	0.002	0.00051	
		010	$H_2{}^{32}S$	–	–	743[b]	320	42	–	0.00038	
			$H_2{}^{34}S$	–	–	240[b]	86	23	–	0.00043	

[a] Including hyperfine constants.
[b] Calculated from experimental energy levels given by Ulenikov et al. [29].
[c] Standard deviation between our measurements and the recorded transitions for each work.

Table 2
Summary of the available data for H_2S pure rotational transitions.

Vib state	Data source		Number of lines				Max. J		Max. K_a		σ[b]
			Total	M		P	M	P	M	P	cm^{-1}
				Microwave	Infrared						
000	HITRAN [18]	$H_2{}^{32}S$	1540	39 [9,13,10,12]	387 [18]	1114	22	27	15	19	0.0062
		$H_2{}^{33}S$	808	1 [9,12]	73 [18]	734	15	22	10	13	0.0008
		$H_2{}^{34}S$	1048	2 [9,12]	173 [18]	873	18	24	12	15	0.0019
	CDMS [23,24]	$H_2{}^{32}S$	1501	82 [11–13,15]	441 [18,19,15]	978	22	25	15	19	0.0037
		$H_2{}^{33}S$	4759[a]	155 [16]	73 [18]	4531	15	22	10	15	–
		$H_2{}^{34}S$	990	40 [12,16]	173 [18]	777	18	24	12	16	0.0009
	JPL [22]	$H_2{}^{32}S$	1525	82 [13,39,15]	379 [19,15]	1064	16	21	13	18	0.0168
	This work	$H_2{}^{32}S$	2919	82 [11–13,15]	1306	1531	26	30	17	20	
		$H_2{}^{33}S$	2471	155 [16]	433	2038	21	32	14	20	
		$H_2{}^{34}S$	2554	40 [12,16]	576	1938	24	28	16	19	
		$H_2{}^{36}S$	1004	1 [16]	91	912	15	17	11	13	
010	This work	$H_2{}^{32}S$	1801		1064	737	22	23	13	16	
		$H_2{}^{34}S$	1083		326	757	14	20	10	12	

[a] Including hyperfine structure.
[b] The standard deviation is calculated using the frequencies measured in this work relative to the results of fits, denoted P for Predicted in each database. M for measured.

Table 3
Parameters in MHz for the (000) vibrational state of $H_2{}^{32}S$, $H_2{}^{33}S$, $H_2{}^{34}S$ and $H_2{}^{36}S$.

	a	Parameter		$H_2{}^{32}S$	$H_2{}^{33}S$	$H_2{}^{34}S$	$H_2{}^{36}S$
1	10 000	A		310 583.5798(106)	310 025.7737(197)	309 502.3997(103)	308 559.20(34)
2	20 000	B		270 367.6824(121)	270 367.1693(224)	270 366.9368(98)	270 354.74(174)
3	30 000	C		141 820.0415(69)	141 702.4070(174)	141 591.8242(93)	141 395.80(93)
4	200	Δ_J		20.861771(261)	20.87749(84)	20.90496(56)	20.6197(151)
5	1100	Δ_{JK}		−76.23237(64)	−76.33674(232)	−76.48005(180)	−73.937(98)
6	2000	Δ_K		117.72636(68)	117.58223(196)	117.49020(147)	115.559(126)
7	40 100	δ_J		8.865995(99)	8.863831(281)	8.866950(141)	8.5716(195)
8	50 000	δ_K		−0.641960(33)	−0.654477(112)	−0.666993(74)	−0.7067(38)
9	300	H_J		0.01022690(312)	0.0100421(84)	0.0102278(111)	
10	1200	H_{JJK}		−0.0903531(127)	−0.089668(58)	−0.091210(55)	
11	2100	H_{JKK}		0.155866(35)	0.154950(126)	0.157519(49)	0.0576(33)
12	3000	H_K		−0.0338364(300)	−0.033831(117)	−0.035149(42)	
13	40 200	h_J	10^{-03}	2.88144(151)	2.8209(39)	2.8646(35)	−3.639(194)
14	50 100	h_{JK}	10^{-03}	−0.96339(71)	−0.97261(229)	−0.98017(188)	−1.1850(286)
15	60 000	h_K	10^{-03}	1.24685(33)	1.25103(125)	1.26596(65)	1.1179(110)
16	400	L_J	10^{-03}	−0.0056700(186)	−0.0040663(291)	−0.005551(71)	0.10398(288)
17	1300	L_{JJK}	10^{-03}	0.072865(181)	0.058824(298)	0.07417(49)	−0.9742(215)
18	2200	L_{JKK}	10^{-03}	−0.22325(78)	−0.18567(146)	−0.20564(95)	1.173(42)
19	3100	L_{JKKK}	10^{-03}	0.27447(96)	0.23823(310)	0.23350(146)	−0.5454(194)
20	4000	L_K	10^{-03}	−0.16145(53)	−0.14806(233)	−0.13911(68)	
21	40 300	l_J	10^{-06}	−1.0205(81)	−0.6487(138)	−1.0517(280)	57.95(177)
22	50 200	l_{JJK}	10^{-06}	−0.2743(37)	−0.2523(93)	−0.2579(98)	
23	60 100	l_{JKK}	10^{-06}	−1.7256(50)	−1.5518(71)	−1.6312(56)	
24	70 000	l_K	10^{-06}	0.39780(137)	0.4483(58)	0.4605(37)	
25	500	M_J	10^{-06}	0.004801(60)		0.003712(147)	−0.3644(167)
26	1400	M_{JJJK}	10^{-06}	−0.06825(128)		−0.04173(149)	3.847(148)
27	2300	M_{JJKK}	10^{-06}	0.2466(58)			−3.981(205)
28	3200	M_{JJKKK}	10^{-06}	−0.4541(77)	−0.0936(105)		1.756(130)
29	4100	M_{JKKKK}	10^{-06}	0.4151(40)	0.1808(240)	0.2908(127)	
30	5000	M_K	10^{-06}	−0.09827(255)	−0.0538(151)	−0.1882(95)	
31	40 400	m_J	10^{-09}	0.8269(141)		0.941(64)	−187.8(86)
32	60 200	m_{JJKK}	10^{-09}	0.7954(275)			
33	70 100	m_{JKKK}	10^{-09}	−0.6732(104)	−0.7882(203)	−1.0281(192)	4.074(302)
34	80 000	m_K	10^{-09}	0.33763(256)	0.3172(123)	0.2162(38)	
35	600	N_J	10^{-09}	−0.003664(90)			
36	1500	N_{JJJK}	10^{-09}	0.07339(253)		−0.02754(260)	−2.857(188)
37	2400	N_{JJKK}	10^{-09}	−0.2464(111)		0.3880(168)	
38	3300	N_{JJKKK}	10^{-09}	0.2604(134)		−0.954(39)	
39	5100	N_{JKKKKK}	10^{-09}	−0.1150(63)		0.2930(165)	
40	50 400	n_{JJJK}	10^{-12}	0.9302(190)	0.5108(216)	0.571(60)	
41	60 300	n_{JJKK}	10^{-12}	−0.509(48)		1.175(57)	
42	70 200	n_{JJKKK}	10^{-12}	0.2140(203)		0.7967(281)	
43	80 100	n_{JKKKK}	10^{-12}	−0.4382(77)	−0.549(34)		
44	90 000	n_K	10^{-12}	0.02109(147)		0.0954(46)	
45	3400	O_{JJJKKK}	10^{-12}			1.205(70)	
46	3500	$P_{JJJJKKK}$	10^{-15}			−1.633(65)	
	110 010 000	X_{aa1}			−32.841(78)		
	110 020 000	X_{bb1}			−8.635(98)		
	10 020 000	C_{bb1}			0.0281(77)		
		σ_{rms}		0.93487	0.93345	0.95080	1.01830

[a] Pickett's program CALPGM notations [35].

predicted up to around 600 cm^{-1}. This predicted spectrum contains 2554 lines with J up to 28 and K_a up to 19. For $H_2{}^{32}S$, 320 newly recorded pure rotational transitions of the vibrational state $\nu_2 = 1$ were used in the fits together with 743 pure rotational transitions calculated from the ν_2 experimental energy levels of Ulenikov et al. [29]. For $H_2{}^{34}S$, the 86 newly recorded transitions were combined with 240 pure rotational transitions calculated from the ν_2 experimental energy levels from the same paper, see Table 2. For $H_2{}^{33}S$, 433 of our measured lines were used together with 155 microwave lines measured by Saleck et al. [16] to fit 31 rotational constants and 3 electric quadrupole hyperfine constants for the ^{33}S nucleus. The predicted spectrum was calculated using

the fitted rotational constants only, *i.e.* neglecting the hyperfine structure. This spectrum contains 2471 lines with J up to 32 and K_a up to 20. Because of the lower abundance of the isotopologue $H_2{}^{36}S$, we were able to detect only 91 transitions, with highest J and K_a values of 15 and 11, respectively. These transitions were combined with a single microwave line published by Saleck et al. [16] to fit 24 rotational parameters.

The presence of the H_2S ortho–para doublets with the 3-to-1 intensity ratio was taken into account in the line assignment process. A value of $\mu = 0.9783$ D [37] for the permanent dipole moment was used in our intensity calculations. This value was used even for transitions within the ν_2 bending mode because no observed value is available for the dipole associated with this state. Our *ab initio* calculations [30] imply that in practice the ν_2 dipole should be about 1% bigger than that for the ground state. For $H_2{}^{32}S$, $H_2{}^{33}S$ and $H_2{}^{34}S$, 296 K partition function values of respectively 503.07, 503.725 and 504.35 [38] are used in our calculations. For $H_2{}^{36}S$, the partition function $Q = 506.51$ was calculated by the CALPGM program. For the intensities of the pure rotational transitions of $H_2{}^{32}S$ and $H_2{}^{34}S$ within their first excited vibrational states $v_2 = 1$, the vibrational band origins from Ref. [29] were used in order to correct the intensity produced by the CALPGM program as given by

$$I = aI_{\mathrm{CALPGM}} e^{-c_2 E_{\mathrm{BO}}/T}, \quad (1)$$

where a is the isotopologue abundance, E_{BO} is the band origin in cm^{-1}, c_2 is the second radiation constant and T is the temperature in K.

The constants obtained from the fits are presented in Tables 3 and 4. The measured and predicted transitions of $H_2{}^{32}S$ and $H_2{}^{34}S$ in their ground and $v_2 = 1$ vibrational states, as well as those for $H_2{}^{33}S$ and $H_2{}^{36}S$ in their ground vibrational states, are given in the Supplementary Material.

Table 4
Parameters in MHz for the (010) vibrational state of $H_2{}^{32}S$ and $H_2{}^{34}S$.

	a	Parameter		$H_2{}^{32}S$	$H_2{}^{34}S$
1	10 000	A		321437.64(67)	320 320.21(128)
2	20 000	B		276 536.85(56)	276 525.06(73)
3	30 000	C		139 967.83(42)	139 744.39(52)
4	200	Δ_J		22.8142(110)	22.9556(119)
5	1100	Δ_{JK}		−84.0407(217)	−84.480(68)
6	2000	Δ_K		138.595(34)	138.641(87)
7	40 100	δ_J		10.3334(42)	10.3734(56)
8	50 000	δ_K		−0.15332(37)	−0.17489(136)
9	300	H_J		0.010084(124)	0.011547(83)
10	1200	H_{JJK}		−0.11031(36)	−0.10671(69)
11	2100	H_{JKK}		0.17914(93)	0.15188(261)
12	3000	H_K		−0.02510(49)	0.0212(37)
13	40 200	h_J	10^{-03}	2.455(55)	3.161(56)
14	50 100	h_{JK}	10^{-03}	−0.70401(264)	−0.6776(149)
15	60 000	h_K	10^{-03}	1.7928(49)	1.7435(130)
16	400	L_J	10^{-03}	0.00930(62)	
17	1300	L_{JJK}	10^{-03}	0.08994(193)	
18	2200	L_{JKK}	10^{-03}		0.237(32)
19	3100	L_{JKKK}	10^{-03}	0.1985(210)	0.311(38)
20	4000	L_K	10^{-03}		−0.933(40)
21	40 300	l_J	10^{-06}	9.518(290)	3.028(197)
22	60 100	l_{JKK}	10^{-06}	−4.442(56)	−2.644(134)
23	500	M_J	10^{-06}	−0.03316(118)	
24	1400	M_{JJJK}	10^{-06}		0.1670(141)
25	2300	M_{JJKK}	10^{-06}	−2.201(34)	
26	3200	M_{JJKKK}	10^{-06}	1.698(71)	−6.545(265)
27	4100	M_{JKKKK}	10^{-06}	−4.188(278)	8.43(34)
28	5000	M_K	10^{-06}	−1.134(87)	
29	40 400	m_J	10^{-06}	−0.02676(55)	
30	60 200	m_{JJKK}	10^{-06}	0.011847(212)	
31	70 100	m_{JKKK}	10^{-09}	3.0862(285)	
32	80 000	m_K	10^{-09}	0.6733(224)	
33	2400	N_{JJJKK}	10^{-09}	4.811(48)	
34	5100	N_{JKKKKK}	10^{-09}	41.08(156)	
35	6000	N_K	10^{-09}	2.80(36)	
36	700	O_J	10^{-12}	−0.11179(197)	
37	6100	$O_{JKKKKKK}$	10^{-12}	−203.3(45)	
38	60 400	o_{JJJKK}	10^{-12}	−0.09893(143)	
39	70 300	o_{JJKKK}	10^{-12}	−0.05405(49)	
40	80 200	o_{JJKKKK}	10^{-15}	−8.75(33)	
41	90 100	o_{JKKKKK}	10^{-15}	4.832(192)	
42	100 000	o_K	10^{-15}	3.725(260)	
43	1700	$P_{JJJJJJK}$	10^{-15}	2.979(53)	
44	3500	$P_{JJJJKKK}$	10^{-15}	−42.39(39)	
45	7100	$P_{JKKKKKKK}$	10^{-15}	382.8(60)	
		σ_{rms}		0.76218	0.86440

[a] Pickett's program CALPGM notations [35].

4. Results and discussion

In this work, more than 2400 lines are recorded for the four isotopologues of H_2S in the ground vibrational state, and for $H_2{}^{32}S$ and $H_2{}^{34}S$ in the first excited bending state. Table 1 summarises the measurements of the H_2S pure rotational spectra from this work and from previous studies. Detailed results for the pure rotational transitions of $H_2{}^{32}S$ and $H_2{}^{34}S$ in their ground and first excited bending states, as well as $H_2{}^{33}S$ and $H_2{}^{36}S$ in their ground states are given in the supplementary material. After a description of the available data used for comparison with this work, results will be detailed.

4.1. Available data

The line positions of the rotational band spectrum collected in HITRAN were originally obtained by Flaud et al. [18] in 1983, who recorded a hydrogen sulfide spectrum between 50 and 310 cm^{-1} with a Fourier transform spectrometer at a resolution of 0.005 cm^{-1}. In this experiment the three isotopic species $H_2{}^{32}S$, $H_2{}^{33}S$, $H_2{}^{34}S$ were observed in natural abundance. Flaud et al. [18] measured 631 lines in this region and combined them with 42 previously published microwave transitions in a least squares fit. Rotational constants for each isotopologue were calculated using the A-I^r representation of the Watson Hamiltonian. These constants were used to predict the positions of the absorption of the natural abundance hydrogen sulfide in the FIR region and intensities using $\mu = 0.974$ D for the permanent dipole moment [10].

In 1994 Yamada and Klee [19] recorded a pure rotational spectrum for $H_2{}^{32}S$ in the FIR region using a Fourier transform infrared spectrometer. They detected more than 370 transitions in the region 30–260 cm^{-1} with a

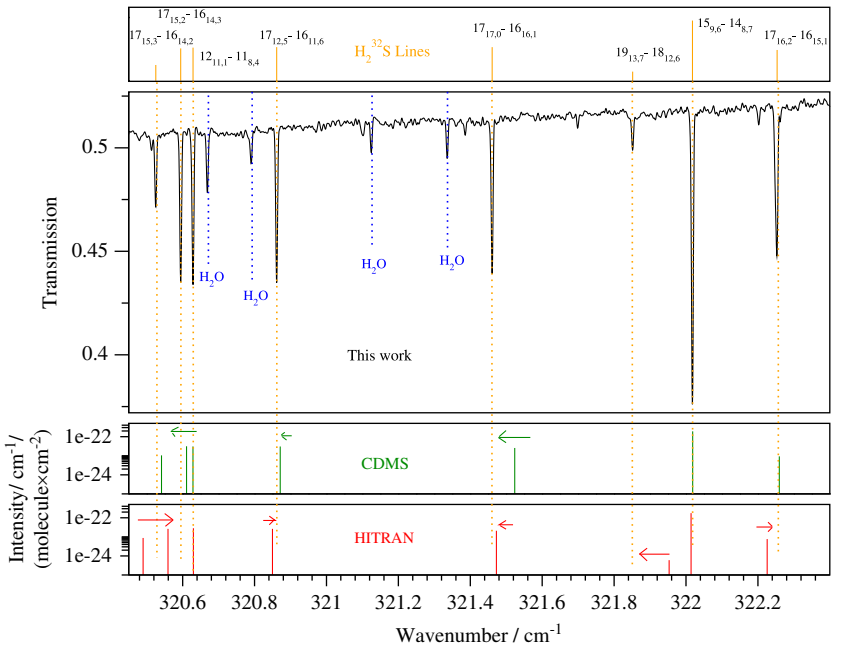

Fig. 4. A portion of the absorption spectrum of H_2S recorded at SOLEIL, showing the errors in the line positions predicted in HITRAN and CDMS databases.

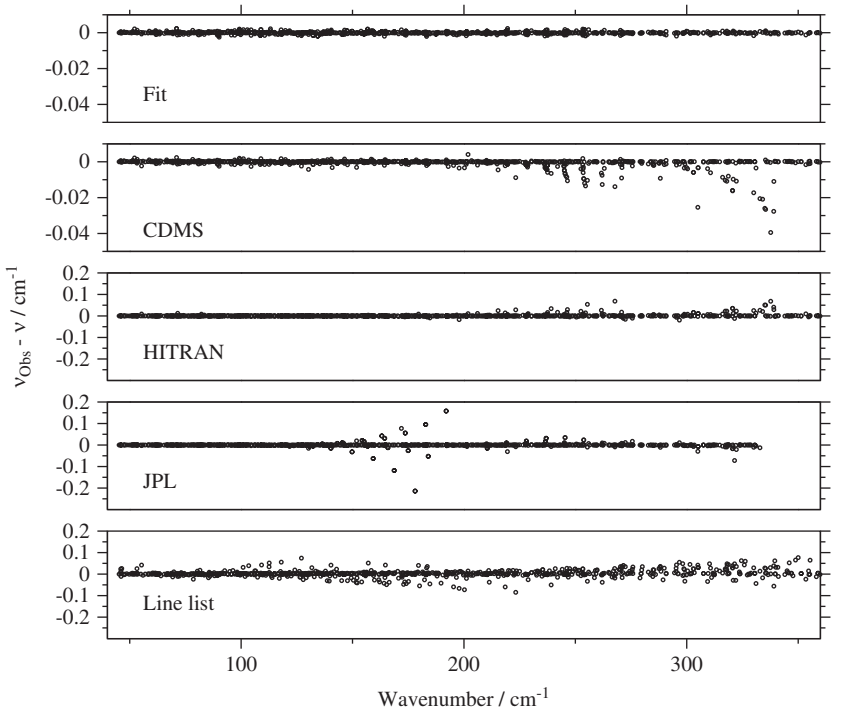

Fig. 5. Accuracy of the ground vibrational state rotational transitions of $H_2{}^{32}S$ in different databases compared to our measurements. $\nu_{Obs}-\nu$ represents the deviations of the line positions measured here from that of CDMS [23], HITRAN [21], JPL [22] and variational calculations [30]. Note the magnified scale for our fit and CDMS.

resolution of 0.0017 cm^{-1}. These lines were combined with the available 40 mm and sub-millimetre wave transition frequencies to test several forms of Watson's reduced Hamiltonian extended up to powers of J[10].

Ground state pure rotational transitions of $H_2{}^{32}S$ were studied by Belov et al. [15] in 1995. They measured rotational transitions frequencies up to 36 cm^{-1} in Cologne and up to 85 cm^{-1} in Lille. The 84 measured lines were analysed

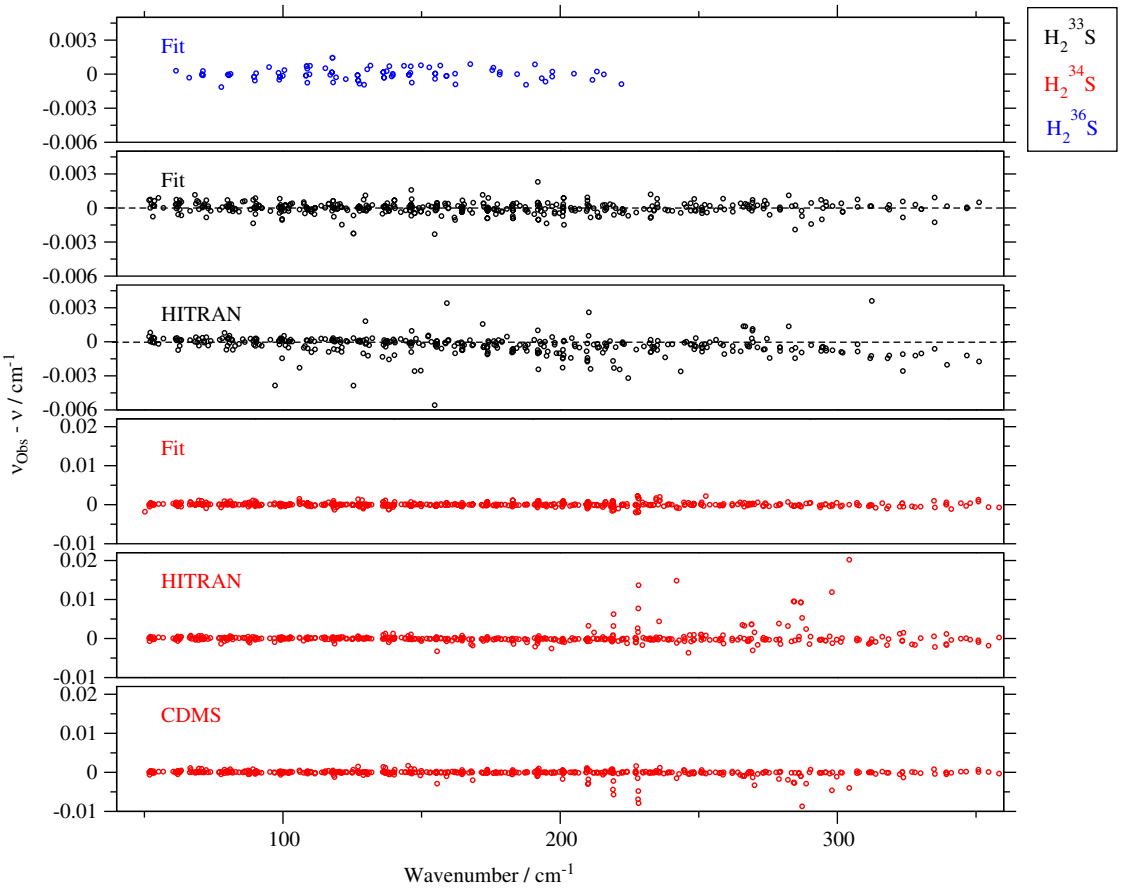

Fig. 6. Accuracy of the ground vibrational state rotational transitions of $H_2{}^{33}S$ and $H_2{}^{34}S$ in our fit, HITRAN [21] and CDMS [23] compared to our measurements. $\nu_{Obs}-\nu$ are given as our observed frequency minus our fit, HITRAN and CDMS. Note the plots for $H_2{}^{34}S$ are on a different vertical scale.

together with the existing microwave and IR data recorded by Yamada and Klee [19] to test a Watson-type Hamiltonian and a Hamiltonian with a Padé formulation [40].

Yamada and Klee's measurements [19] were subsequently combined with the measurements by Helminger et al. [13,15] and Belov et al. [39] to predict the $H_2{}^{32}S$ pure rotational lines which are in the JPL catalogue [22] for J up to 21 using $\mu=0.974$ D [10]. The data published in CDMS catalogue was predicted for $H_2{}^{32}S$ up to $J=25$, $H_2{}^{33}S$ up to $J=22$, and $H_2{}^{34}S$ up to $J=24$ using the measurements from Refs. [11–13,18,19,15] and $\mu=0.9783$ D [37].

The most accurate study of lines positions in the ν_2 band of H_2S was performed by Ulenikov et al. [29]. In this work, lines were assigned to $H_2{}^{32}S$ and its isotopologues $H_2{}^{33}S$ and $H_2{}^{34}S$ with a resolution of 0.0020 cm^{-1}. 226 upper state energy levels were obtained with $J\leq17$ and $K_a\leq13$ for $H_2{}^{32}S$. 181 of these energy levels up to $J\leq17$ and $K_a\leq10$ were fitted with a standard deviation of 9.96×10^{-5} cm^{-1}. For $H_2{}^{34}S$, 126 energy levels with $J\leq14$ and $K_a\leq10$ were obtained, 80 of them up to $J\leq12$ and $K_a\leq7$ were used to fit the constants for the $v_2=1$ vibrational state of this isotopologue. Ulenikov et al. [29] used the ground state energies for the three isotopologues from Ref. [18].

Table 5
Three $H_2{}^{36}S$ rotational transitions published by Saleck et al. [16] and their counterparts calculated in this work. The numbers in parentheses next to Saleck et al. and This work transition values are the experimental uncertainty and the fitting estimated error, respectively. Δ is the difference between the transitions in the two works.

$J'_{K_aK_c}-J''_{K_aK_c}$	Saleck et al. (MHz)	This work (MHz)	Δ (MHz)
$3_{3,1}-3_{2,2}$	559 250.950 (0.100)	559 796 (27)	−546
$4_{4,1}-4_{3,2}$	636 677.520 (0.100)	637 643 (37)	−966
$2_{0,2}-1_{1,1}$	686 766.635 (0.100)[a]	686 772 (24)	−6

[a] Line included in our fit.

4.2. Rotational transitions in the ground vibrational state

As can be seen from Table 1, we were able to extend significantly the number of the experimental infrared lines for all the four isotopologues of H_2S considered. For instance, for the transitions within the ground vibrational state of $H_2{}^{32}S$, we recorded 926 lines, while only 387 lines from the same spectral region were reported by Flaud et al. [18]. Our spectrum contains lines with J up to 26 and K_a up to 17, which also significantly extends the coverage of the energy levels probed, see Table 1. This table also

shows standard deviations between our measured line positions and the previously measured line positions. Our analysis suggests that while we get very good agreement with the previous measurements, but there are problems with the predicted line positions tabulated in the databases, see Table 2. Fig. 4 illustrates some of these errors in

Table 6
Summary of the differences in the predicted line positions, in cm^{-1}, in different databases compared to the measured line positions of this work.

Vib. state transition	ISO	Data source	Max. absolute error	error > 0.001 cm^{-1}		Number of lines
				Min. J	Min. K_a	errors > 0.001 cm^{-1}
000–000	$H_2{}^{32}S$	HITRAN	0.0687	3	1	213
		CDMS	0.0626	3	2	139
		JPL	0.2141	3	2	238
		This work	0.0025	4	0	105
		Line list [30]	0.0848	3	3	780
	$H_2{}^{33}S$	HITRAN	0.0056	2	0	124
		This work	0.0023	6	1	30
	$H_2{}^{34}S$	HITRAN	0.0202	6	1	62
		CDMS	0.0087	6	1	40
		This work	0.0022	6	1	35
	$H_2{}^{36}S$	This work	0.0014	10	1	3
010–010	$H_2{}^{32}S$	This work	0.0023	9	2	18
		Line list [30]	0.3695	2	1	203
	$H_2{}^{34}S$	This work	0.0024	7	3	10

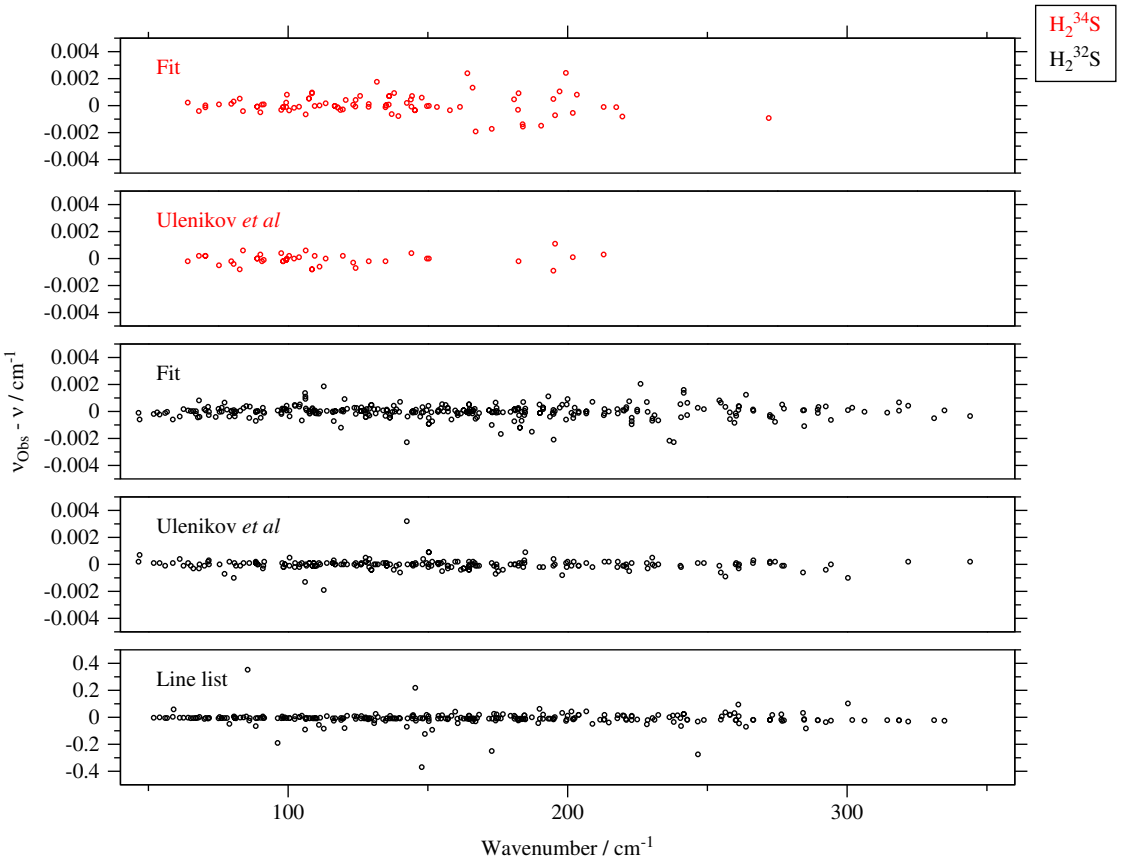

Fig. 7. Accuracy of the first bending vibrational state pure rotational transitions of $H_2{}^{32}S$ and $H_2{}^{34}S$ in our fit, and the transitions calculated from the experimental energy levels published by Ulenikov et al. [29] compared to our measurements. Also the variational calculations [30] compared to our measurements for $H_2{}^{32}S$. $\nu_{Obs}-\nu$ given as our observed frequency minus our fit, Ulenikov et al.'s transitions, and the variational calculations. Note the reduced scale for the line list.

the prediction of the lines positions in the HITRAN and CDMS databases; Table 6 summarises these problems. Figs. 5 and 6 give general idea about the accuracy of the line positions available in these databases and those from our fit.

Rotational transitions of the $H_2{}^{36}S$ isotopologue in its ground vibrational state are detected in this work up to $J=15$ and $K_a=11$. Over 50 lines were identified and assigned manually by the extrapolation method mentioned above. As a result, 91 lines were assigned as $H_2{}^{36}S$ lines with a root mean square error of 0.00051 cm^{-1}. Saleck et al. [16] published three recorded microwave lines as $H_2{}^{36}S$ rotational transitions. From these lines, only the transition $2_{0,2}-1_{1,1}$ at 686 766.635 MHz could be added to our fit without destroying it. These three transitions are listed in Table 5 and compared to the predicted line positions resulting from our fit.

4.3. Rotational transitions in the bending vibrational state $v_2=1$ of $H_2{}^{32}S$ and $H_2{}^{34}S$

We were able to assign initially 214 pure rotational transitions associated with the vibrational state $v_2=1$ of $H_2{}^{32}S$ covering energy levels up to $J=20$ and $K_a=14$ using the variationally calculated line list. Then 181 experimental energy levels up to $J\leq17$ and $K_a\leq10$ from Ref. [29] were used to calculate 759 rotational transitions in the first excited bending state for $H_2{}^{32}S$. 559 of these calculated transitions are in the region 45–360 cm^{-1}. The calculations were performed using the combination differences method. As a result, 216 transitions could be matched to transitions in our spectrum with the standard deviation of 0.0004 cm^{-1}. Eight lines were found to have much higher errors in their calculated positions (all close to 0.3 cm^{-1}). All these lines belong to the energy levels $12_{2,11}$ and $12_{1,11}$, and all the calculated transitions involving these energy levels showed the same problem during the fit. We suspect that this is a typographical problem in the corresponding table of Ref. [29]. However these transitions were excluded from the fit; they are tabulated in the Supplementary Material. Our spectrum contains 104 transitions that cannot be calculated from Ulenikov et al.'s experimental energy levels. These new recorded transitions have quantum numbers up to $J=22$ and $K_a=13$. Fig. 7 shows the accuracy of the fit performed in this work for $H_2{}^{32}S$ rotational spectrum in the $v_2=1$ state as well as the calculated rotational transitions using the experimental energy levels of Ulenikov et al. [29] and the variationally calculated line list.

For $H_2{}^{34}S$, 240 rotational transitions up to $J=12$ and $K_a=7$ were calculated using the 80 experimental energy levels published by Ulenikov et al. [29]. 177 lines of these calculated transitions are in the region 45–360 cm^{-1}. 42 lines could be assigned in our spectrum using these calculated transitions for $J\leq10$ and $K_a\leq6$. After fitting the effective Hamiltonian constants, 44 extra lines were assigned up to $J=14$ and $K_a=10$. Fig. 7 shows the accuracy of the fit for $H_2{}^{34}S$ pure rotational spectrum in the $v_2=1$ state and the calculated pure rotational transitions using the experimental energy levels of Ulenikov et al. [29].

Fig. 2 shows a portion of the assigned spectrum which includes transitions for the four isotopologues of H_2S with the same quantum numbers and some pure rotational $v_2=1$ transitions of $H_2{}^{32}S$ and $H_2{}^{34}S$.

5. Conclusions

More than 1300 new lines in the pure rotational band of the absorption spectrum for $H_2{}^{32}S$, $H_2{}^{33}S$, $H_2{}^{34}S$, and $H_2{}^{36}S$ are detected and assigned in the ground vibrational state as well as in the first excited bending vibrational state for $H_2{}^{32}S$ and $H_2{}^{34}S$. Using these newly detected lines, the effective rotational constants for the four isotopologues of H_2S in the two vibrational states are fitted. Problems in predicted line positions from CDMS, and JPL databases made on the basis previous studies were identified. Our new data has been submitted for inclusion in the 2012 update of the HITRAN database [41].

Acknowledgements

We thank Olga Naumenko and an anonymous referee for helpful comments on our manuscript, and Oleg Polyansky for helpful discussions during the course of this work. Ala'a Azzam thanks the University of Jordan for financial support. This work is partially supported by ERC Advanced Investigator Project 267219.

Appendix A. Supplementary data

Supplementary data associated with this article can be found in the online version at http://dx.doi.org/10.1016/j.radphyschem.2011.02.020.

References

[1] Hoshyaripour G, Hort M, Langmann B. How does the hot core of a volcanic plume control the sulfur speciation in volcanic emission? Geochem Geophys Geosyst 2012;13:Q07004.
[2] Llavador Colomer F, Espinos Morato H, Mantilla Iglesias E. Estimation of hydrogen sulfide emission rates at several wastewater treatment plants through experimental concentration measurements and dispersion modeling. J Air Waste Manage Assoc 2012;62:758–66.
[3] Visscher C, Lodders K, Fegley Jr. B. Atmospheric chemistry in giant planets, brown dwarfs, and low-mass dwarf stars. II. Sulfur and phosphorus. Astron Astrophys 2006;648:1181–95.
[4] Zahnle K, Marley MS, Freedman RS, Lodders K, Fortney JJ. Atmospheric sulfur photochemistry on hot jupiters. Astrophys J 2009;701:L20–4.
[5] Thaddeus P, Wilson RW, Kutner ML, Jefferts KB, Penzias AA. Interstellar hydrogen sulfide. Astrophys J 1972;176:L73.
[6] Aladro R, Martin S, Martin-Pintado J, Mauersberger R, Henkel C, Ocana Flaquer B, et al. A $\lambda=1.3$ mm and 2 mm molecular line survey towards M 82. Astron Astrophys 2011;535:A84.
[7] Wakelam V, Castets A, Ceccarelli C, Lefloch B, Caux E, Pagani L. Sulphur-bearing species in the star forming region L1689N. Astron Astrophys 2004;413:609–22.
[8] Justtanont K, Khouri T, Maercker M, Alcolea J, Decin L, Olofsson H, et al. Herschel/hifi observations of o-rich agb stars: molecular inventory. Astron Astrophys 2012;537:A144.
[9] Burrus CA, Gordy W. One-to-two millimeter wave spectroscopy. II. H_2S. Phys Rev 1953;92:274–7.
[10] Huiszoon C, Dymanus A. Magnetic hyperfine structure the rotational spectrum of H_2S. Phys Lett 1966;21:164–6.

[11] Cupp RE, Keikpf RA, Gallagher JJ. Hyperfine structure in the millimeter spectrum of hydrogen sulfide electric spectroscopy on asymmetric-top molecules. Phys Rev 1968;171:60–9.
[12] Huiszoon C. A high resolution spectrometer for the shorter millimeter wavelength region. Rev Sci Instrum 1971;42:477–81.
[13] Helminger P, Cook RL, De Lucia FC. Microwave spectrum and centrifugal distortion effects of H_2S. J Chem Phys 1972;56:4581–4.
[14] Burenin AV, Fevralskikh TM, Melnikov AA, Shapin SM. Microwave spectrum of the hydrogen sulfide molecule $H_2{}^{32}S$ in the ground state. J Mol Spectrosc 1985;109:1–7.
[15] Belov SP, Yamada KMT, Winnewisser G, Poteau L, Bocquet R, Demaison J, et al. Terahertz rotational spectrum of H_2S. J Mol Spectrosc 1995;173:380–90.
[16] Saleck AH, Tanimoto M, Belov SP, Klaus T, Winnewisser G. Millimeter- and submillimeter-wave rotational spectra of rare hydrogen sulfide isotopomers. J Mol Spectrosc 1995;171:481–93.
[17] Miller RE, Leroi GE, Hard TM. Analysis of the pure rotational absorption spectra of hydrogen sulfide and deuterium sulfide. J Chem Phys 1969;50:677–84.
[18] Flaud J-M, Camy-Peyret C, Johns JWC. The far-infrared spectrum of hydrogen-sulfide—the (000) rotational-constants of $H_2{}^{32}S$, $H_2{}^{33}S$ and $H_2{}^{34}S$. Can J Phys 1983;61:1462–73.
[19] Yamada KMT, Klee S. Pure rotational spectrum of H_{2S} in the far-infrared region measured by ftir spectroscopy. J Mol Spectrosc 1994;166:395–405.
[20] Rothman LS, Jacquemart D, Barbe A, Benner DC, Birk M, Brown LR, et al. The HITRAN 2004 molecular spectroscopic database. J Quant Spectrosc Radiat Transfer 2005;96:139–204.
[21] Rothman LS, Gordon IE, Barbe A, Benner DC, Bernath PF, Birk M, et al. The HITRAN 2008 molecular spectroscopic database. J Quant Spectrosc Radiat Transfer 2009;110:533–72.
[22] Pickett HM, Poynter RL, Cohen EA, Delitsky ML, Pearson JC, Muller HSP. Submillimeter, millimeter, and microwave spectral line catalog. J Quant Spectrosc Radiat Transfer 1998;60:883–90.
[23] Müller HSP, Thorwirth S, Roth DA, Winnewisser G. The cologne database for molecular spectroscopy, CDMS. Astron Astrophys 2001;370:L49–52.
[24] Müller HSP, Schlöder F, Stutzki J, Winnewisser G. The cologne database for molecular spectroscopy, CDMS: a useful tool for astronomers and spectroscopists. J Mol Struct (Theochem) 2005;742:215–27.
[25] Kozin IN, Jensen P. Fourfold clusters of rotational energy levels for H_2S studied with a potential energy surface derived from experiment. J Mol Spectrosc 1994;163:483–509.
[26] Lane WC, Edwards TH, Gillis JR, Bonomo FS, Murcray FJ. Analysis of ν_2 of H_2S. J Mol Spectrosc 1982;95:365–80.
[27] Strow LL. Line strength measurements using diode laser: the ν_2 band of H_2S. J Quant Spectrosc Radiat Transfer 1983;29:395–406.
[28] Lane WC, Edwards TH, Gillis JR, Bonomo FS, Murcray FJ. Analysis of ν_2 of $H_2{}^{33}S$ and $H_2{}^{34}S$. J Mol Spectrosc 1985;111:320–6.
[29] Ulenikov ON, Malikova AB, Koivusaari M, Alanko S, Anttila R. High resolution vibrational.rotational spectrum of H_2S in the region of the ν_2 fundamental band. J Mol Spectrosc 1996;176:229–35.
[30] Azzam AAA, Yurckenko SN, Tennyson J. ExoMol Molecular linelists: III A linelist for the hydrogen sulphide molecule. Mon Not R Astr Soc; 2013 (in preparation).
[31] Brubach J-B, Manceron L, Rouzières M, Pirali O, Balcon D, Kwabia-Tchana F, et al. Performance of the AILES THz-Infrared beamline at SOLEIL for High resolution spectroscopy. In: WIRMS 2009, AIP conference proceedings, vol. 1214; 2010, p. 81–4.
[32] Matsushima F, Odashima H, Iwasaki T, Tsunekawa S, Takagi K. Frequency-measurement of pure rotational transitions of H_2O from 0.5 to 5 THz. J Mol Struct 1995;352:371–8.
[33] Horneman VM, Anttila R, Alanko S, Pietila J. Transferring calibration from CO_2 laser lines to far infrared water lines with the aid of the ν_2 band of OCS and the ν_2, $\nu_1-\nu_2$, and $\nu_1+\nu_2$ bands of $^{13}CS_2$: molecular constants of $^{13}CS_2$. J Mol Spectrosc 2005;234:238–54.
[34] Tennyson J, Kostin MA, Barletta P, Harris GJ, Polyansky OL, Ramanlal J, et al. DVR3D: a program suite for the calculation of rotation-vibration spectra of triatomic molecules. Comput Phys Commun 2004;163:85–116.
[35] Pickett HM. The fitting and prediction of vibration-rotation spectra with spin interactions. J Mol Spectrosc 1991;148:371–7.
[36] Huiszoon C, Dymanus A. Stark effect of millimeter wave transitions, I. hydrogen sulfide. Physica 1965;31:1049–52.
[37] Viswanathan R, Dyke TR. Electric dipole moments and nuclear hyperfine interactions for H_2S, HDS, and D_2S. J Mol Spectrosc 1984;103:231–9.
[38] Šimečková M, Jacquemart D, Rothman LS, Gamache RR, Goldman A. Einstein A coefficients and statistical weights for molecular absorption transitions in the HITRAN database. J Quant Spectrosc Radiat Transfer 2006;98:130–55.
[39] Helminger P, De Lucia FC, Kirchhoff WH. Microwave spectra of molecules of astrophysical interest iv. hydrogen sulfide. J Phys Chem Ref Data 1973;2:215–23.
[40] Polyansky OL. One-dimensional approximation of the effective rotational hamiltonian of the ground-state of the water molecule. J Mol Spectrosc 1985;112:79–87.
[41] Rothman LS, Gordon IE, Babikov Y, Barbe A, Benner DC, Bernath PF, et al. The HITRAN database: 2012 edition. J Quant Spectrosc Radiat Transfer 2013, in this issue.